Lessons from Engineering: A Live Demonstration of the ATRIAS Biped

Walking and Running with Passive Compliance

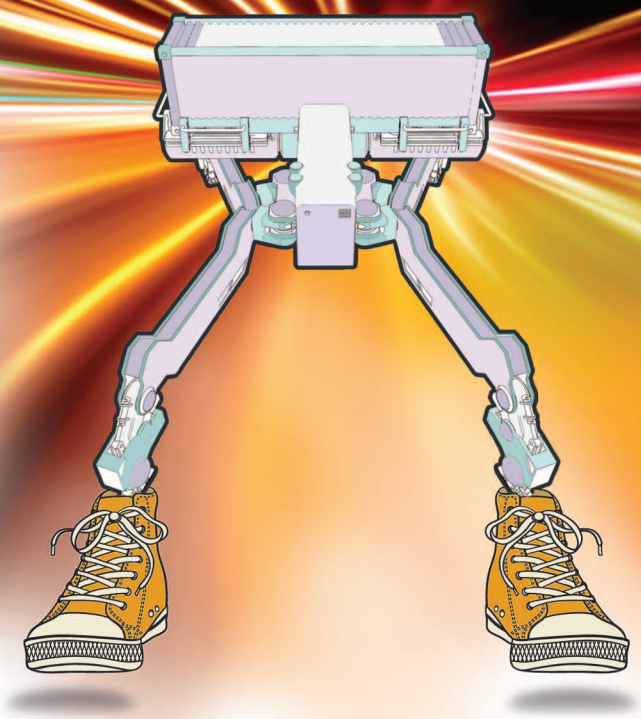

ROBOT: ©ISTOCKPHOTO.COM/LEAFEDGE
SNEAKERS—©ISTOCKPHOTO.COM/ SNTPZH
BACKGROUND—IMAGE LICENSED BY INGRAM PUBLISHING

By Christian Hubicki, Andy Abate, Patrick Clary, Siavash Rezazadeh, Mikhail Jones, Andrew Peekema, Johnathan Van Why, Ryan Domres, Albert Wu, William Martin, Hartmut Geyer, and Jonathan Hurst

Biological bipeds have long been thought to take advantage of compliance and passive dynamics to walk and run, but realizing robotic locomotion in this fashion has been difficult in practice. Assume The Robot Is A Sphere (ATRIAS) is a bipedal robot designed to take advantage of the inherent stabilizing effects that emerge as a result of tuned mechanical compliance (Table 1). In this article, we describe the mechanics of the biped and how our controller exploits the interplay between passive dynamics and actuation to achieve robust locomotion. We outline our development process for the incremental design and testing of our controllers through rapid iteration.

By show time at the Defense Advanced Research Projects Agency (DARPA) Robotics Challenge (Figure 1), ATRIAS was able to walk with robustness, locomote in terrain from asphalt to grass to artificial turf, and traverse changes in surface height as large as 15 cm without planning or visual feedback. Furthermore, ATRIAS can accelerate from rest, transition smoothly to a running gait, and reach a top speed of 2.5 m/s (9 km/h). Reliably achieving such dynamic locomotion in an uncertain environment required rigorous development and testing of the hardware, software, and control algorithms. This endeavor culminated in seven live shows of ATRIAS walking and running, with disturbances and without falling, in front of a live audience at the DARPA Robotics Challenge.

Approaches to Biped Control

Walking and running on two legs is an enduring challenge in robotics. Avoiding falls becomes especially tricky when the terrain is uncertain in both its geometry and rigidity. A promising approach to achieving stable control is to relinquish some authority to purposeful passive dynamics, perhaps by adding mechanical compliance [1] or removing actuators entirely [2]. If the machine's unactuated dynamics are thoughtfully designed, they can passively attenuate disturbances and require smaller adjustments from the controller [33].

Digital Object Identifier 10.1109/MRA.2017.2783922
Date of publication: 10 May 2018

The ATRIAS biped [3] is a physical embodiment of this mechanical intelligence approach [24], equipped with four degrees of passive compliance in its legs and motor-free pin joints for feet. While eschewing actuators and inserting springs make control less formally tractable [4], we found that thoughtfully applying insights from reduced-order models [5] can yield a range of agile and stable locomotion behaviors. In doing so, we aimed to demonstrate that three-dimensional (3-D) bipedal walking and running are not only possible with a passive-dynamics-based approach, but that the result is sufficiently robust to serve as a viable framework for practical locomotion in unstructured environments.

Table 1. The specifications of the ATRIAS bipedal robot.

ATRIAS at a Glance	
Top speed	2.5 m/s
Maximum ground height variation	15 cm
Maximum kick impulse	60 kg·m/s
Surface incline	15°
Airborne time per step while running	30 ms
Mechanical cost of transport	1.0
Total cost of transport	1.3
Battery life	30 min
Leg length	1.0 m
Height	1.7 m
Weight	60 kg
Spring stiffness	3 kN·m/rad
Leg stiffness at 0.9-m rest length	20 kN/m
Control rate	1.0 kHz
Lines of controller code	880

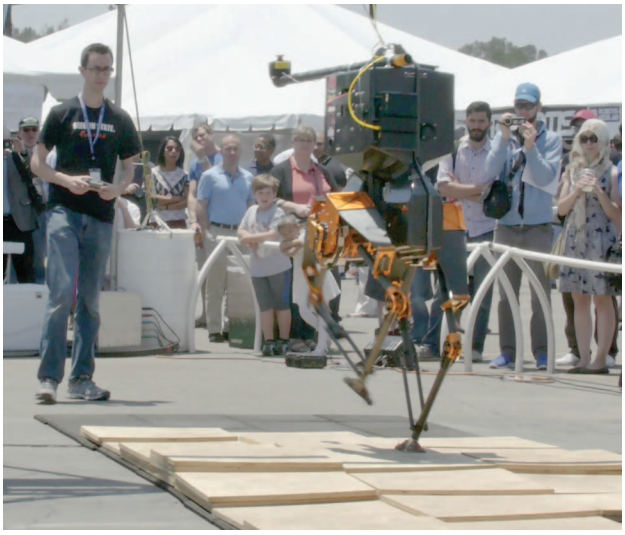

Figure 1. The ATRIAS bipedal robot performing one of its seven live dynamic demonstrations in front of a live audience at the DARPA Robotics Challenge. For one component of the show, the spring-legged robot walked over uneven surfaces without visual sensing or external support.

Zero moment point (ZMP) approaches have long been the go-to methods for generating stable bipedal locomotion [6]. The core strategy of maintaining full actuation through flat-footed contact is at the heart of the field's most visible humanoids, including ASIMO, HUBO, and the HRP-series humanoids [7], [8], [22]. Given ZMP's track record of success, elaborations of this basic concept [9] were ubiquitous at the high-stakes DARPA Robotics Challenge [10], [20], [28], [40], [47], [48]. However, these approaches require planning with respect to the environment to ensure ZMP criteria. As terrain becomes less structured and locomotion becomes faster, it becomes more difficult to rely on planning for locomotion stability.

In contrast to a planning approach, researchers have also studied locomotion as a potentially self-stable phenomenon [39]. Using reduced-order spring-mass models [11], they have developed locomotion strategies to mitigate [12] or entirely reject disturbances without feedback [13]. These passively compliant models and corresponding simple control strategies theoretically have been extended across walking and running [30], [34]. These math models, while simple, are sufficiently relevant to biological locomotion that they are commonly used to analyze stabilization in animal locomotion [26], [29], [32], [35]. As with animals, our robot will not precisely match these simple math models, but we may use the insights from and general behaviors of spring-mass systems to guide the control policies of our robot toward self-stability.

Likely the most famous examples of insight-driven biped control were the Raibert hoppers [1] and their successors [14], which were amazingly agile but required power through an offboard pneumatic tether. Other examples include the hyperefficient walkers [15] and [16], which also had control designed to work effectively with their passive dynamics. Recognizing some merit to passive dynamics and compliance, some engineers have begun to develop formal approaches to the challenge of underactuation in robotics [41], [43]. Variations on methods such as hybrid zero dynamics [46] have been successful in achieving planar walking, both with compliance [17], [18], [31] and without [19], as well as running [42] and preliminary walking implementation in 3-D [36]. Other methods have begun to show promise in simulation for achieving robust bipedal running [21], [45].

Our specific goal at the DARPA Robotics Challenge was to exhibit robust walking and running on unstructured terrain with all components, including batteries, onboard the machine. The purpose was to demonstrate the practical potential of this compliant approach to bipedal locomotion. With these soft spring-leg mechanisms, we were able both to walk and smoothly accelerate up to running speeds (2.5 m/s). The dynamic approach to stability allowed ATRIAS to recover from large unmodeled impulses (i.e., kicks). Furthermore, we demonstrated walking on uneven ground without any vision or preparative planning, including 15-cm steps and nonrigid terrain. The resulting locomotion was also energy efficient compared to bipeds of similar scale, with a total cost of transport (TCoT) of 1.3. (Cost of transport, either mechanical or total, is a nondimensional metric of energy economy,

representing energy cost per unit robot weight per unit distance. ASIMO is estimated to have a TCoT of 3.2 [37].)

Robot Overview

ATRIAS is designed to perform highly dynamic walking and running gaits. Complementary passive hardware, a mechanism that is just as dynamic as the locomotion itself, allows the biped to be reactive and stable when disturbed. Because the hardware and algorithms are equal partners in generating the locomotion patterns, the method used to control ATRIAS would not function without the intended natural dynamics built into the mechanisms.

Mechanical Overview

Even with pantograph legs unlike anything seen in nature, ATRIAS performs bouncy gaits and reacts to trips and falls in a convincingly natural way. Its construction is the result of an effort to reproduce the natural dynamics and passive responses found in nature rather than to mimic any particular morphology [3]. Figure 2 shows the full biped robot, highlighting

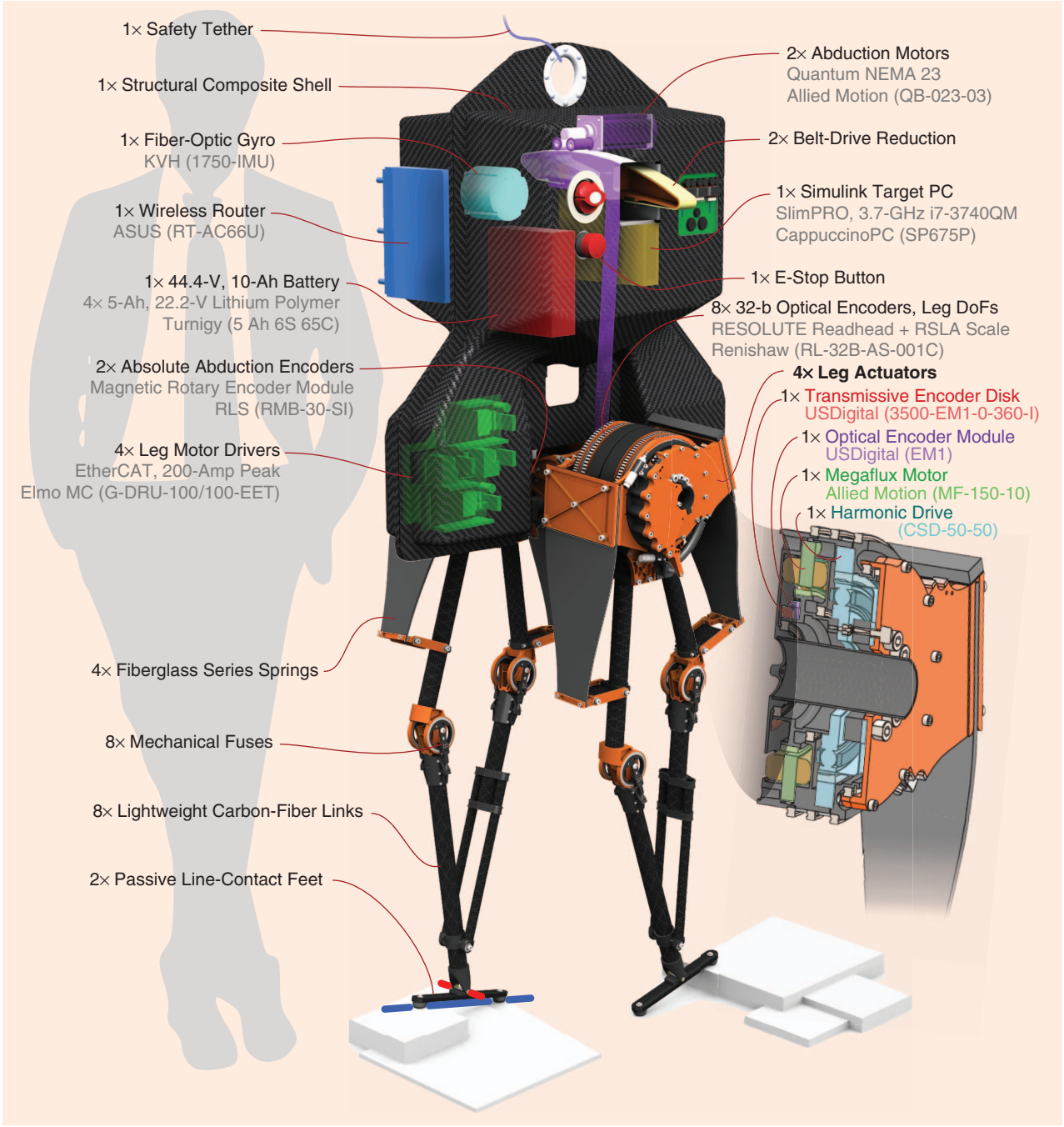

Figure 2. A rendered view of ATRIAS with mechanisms and features highlighted. Most systems are located in the composite torso, with only the actuation and sensing on the legs. Part numbers and suppliers are provided for selected components. E-Stop: emergency stop. (Figure courtesy of Andy Abate.)

important components and providing references to product part numbers.

Many animals, including humans, have walking and running gaits that can be described by springy, mathematically simple legs. A common spring-mass model is the spring-loaded inverted pendulum (SLIP) model, with a point-mass body, a massless point toe, and a massless linear spring connecting the two. When in contact with the ground, the toe is assumed to be in perfect contact and completely fixed. When leg forces drop to zero, the toe is no longer fixed to the ground and moves rigidly with the point mass. This model is completely energy conservative, because the toe is massless and there is a massless spring between the toe contact and the point mass; it can walk or run continuously as long as the average ground height is consistent.

Observers can see the influence of spring-mass models in the ATRIAS design: carbon-fiber legs for minimum inertia connected by series springs to the concentrated mass at the hips. Such construction gives the biped noticeably SLIP-like dynamics (Figure 3). With series compliance, unforeseen effects are softened, and energy can be recycled from step to step and released at higher rates than the motor alone can deliver. These combined factors have the potential to improve the robustness of the mechanism as well as energy efficiency.

Kinematically, ATRIAS has two planar legs comprising a parallel mechanism, two actuators colocated at the hip, and a distal toe. Each leg has an abduction degree of freedom (DoF), with both sharing an axis in the sagittal plane of the torso. Six total actuators exist on the robot: two legs, each with hip extension, knee extension, and hip abduction. (Note that ATRIAS has 13 DoF and thus is heavily underactuated for a bipedal robot.) The robot lacks long-axis rotation of the hip and thus cannot actively turn.

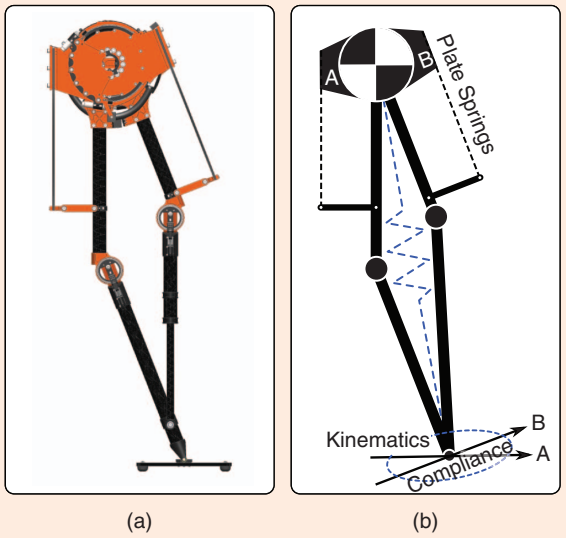

Figure 3. (a) A rendered view of the ATRIAS leg design. (b) A schematic view showing the kinematics and compliant behavior of the toe. The basis vectors of motors A and B are drawn at the toe to illustrate the kinematics of this pose. The instantaneous motion of the toe is the weighted sum of these basis vectors. Similarly, a compliance ellipse shows the elastic behavior of the physical toe around the neutral point [25]; the ellipse represents the deflection of the toe for a unit force in all directions, so the major axis is soft and the minor axis is stiff. (Figure courtesy of Andy Abate.)

A passive foot is attached at the ankle in a way that simulates a point contact at the ground but restricts yaw rotation, thereby removing this DoF from the dynamics of the robot. The two-point line contacts at the bottom of the feet keep ATRIAS pointed in roughly the same direction between steps by providing frictional contact with the ground [23].

Mechanical fuses at the knees protect the robot from damage due to excessive sideloads at the toe. This resistance to significant damage makes rapid iteration and testing possible. Expensive and difficult repairs to bearings, the transmission, and the carbon-fiber legs would halt progress, but fuses are easy to reattach.

Because ATRIAS is a prototype experimental platform, it is fairly fragile and cannot withstand torso collisions or falls. A portable gantry system protects the robot from falls via a safety line. During operation, the line is kept slack so as to not affect the robot's dynamics unless it drops or goes wildly off course. ATRIAS is otherwise entirely self-contained, and this connection is meant to catch the robot only in the event of a malfunction.

Electrical/Software Overview

ATRIAS's electrical architecture is built around commodity personal computer (PC) hardware, custom sensor interface boards, and off-the-shelf motor drivers. An EtherCAT data bus provides high-throughput, offers real-time communication between the system components, and interfaces directly with the Simulink real-time operating system. Commercial off-the-shelf (COTS) lithium polymer batteries power the motor drivers as well as the computer and other components through COTS dc–dc voltage regulation modules. Figure 4 shows the major components of the electrical system.

All control processing is done with an onboard miniature desktop computer. This device is a commercially available small-form-factor PC based on a modern Intel desktop processor. The robot computer executes our control software, developed in MATLAB and Simulink, on top of the Simulink Real-Time kernel. The Simulink kernel ships with drivers for using the EtherCAT protocol with standard Ethernet chipsets, which are used to retrieve sensor data and send torque commands to the motor drivers.

ATRIAS's six motors are driven with two different types of motor amplifier. The hip extension and knee extension motors use EtherCAT-enabled COTS servo drivers capable of supplying a peak current of 200 A. The hip abduction motors are driven by smaller COTS motor drivers able to deliver a peak current of 60 A. All of these drive three-phase brushless motors in current-control mode, using Hall effect sensors and an incremental encoder for sinusoidal commutation.

ATRIAS uses only proprioceptive sensing for control and is otherwise blind to the environment. High-resolution

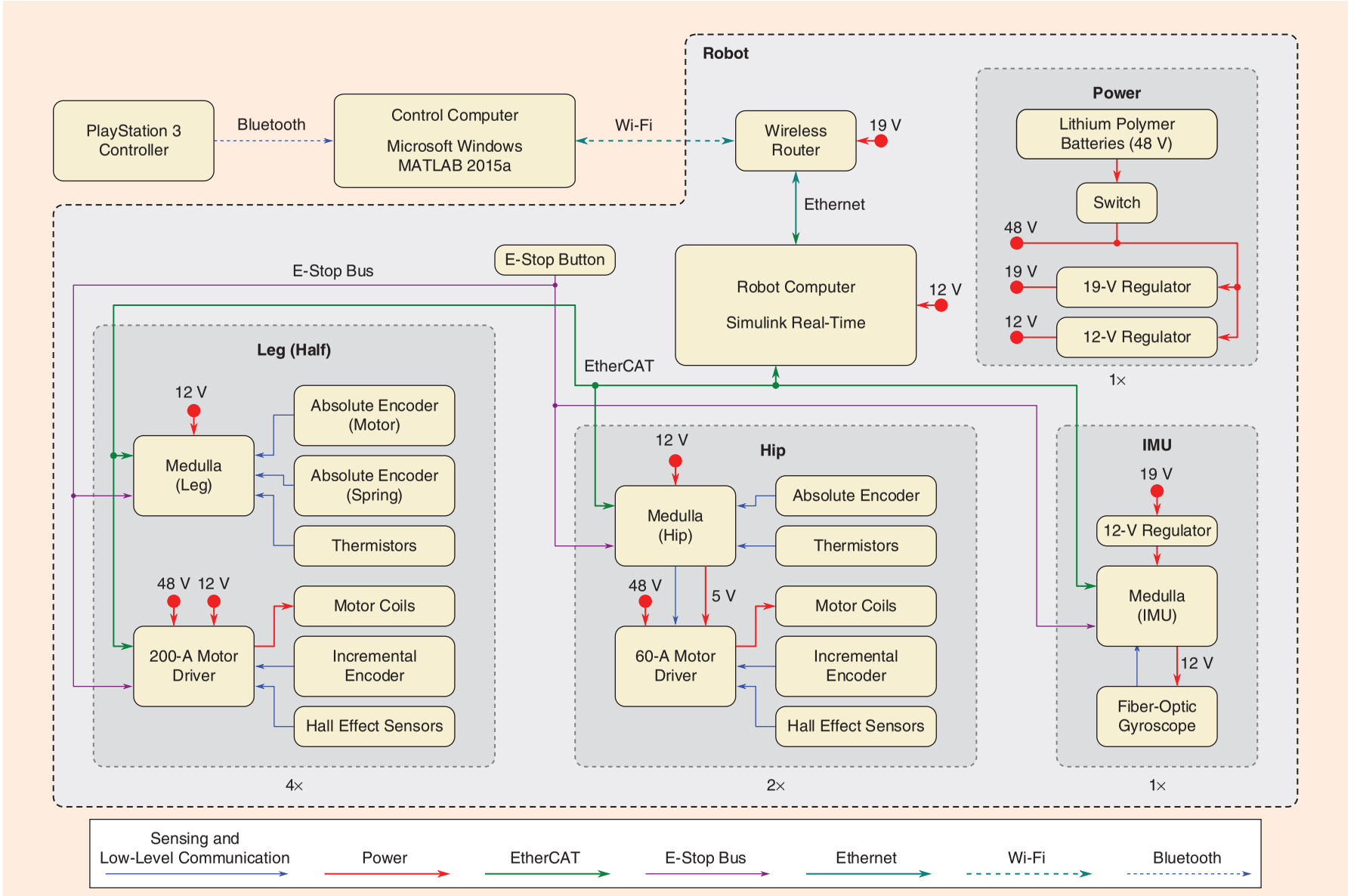

Figure 4. A connection diagram of the electrical system.

absolute encoders at each internal DoF provide joint angles and spring deflections, and a fiber-optic gyroscope provides torso orientation. These sensors are sufficient to determine the configuration of the robot, save for its translation with respect to the world frame.

Custom, versatile interface modules, called *Medulla* modules, read, translate, packetize, and send proprioceptive and orientation sensor data to the control computer. The Medullas also read thermistors embedded in the motor assemblies so the controller can detect and respond to overheating. Some Medulla modules are used to pass torque commands to the hip abduction motor drivers, as these cannot connect directly to the EtherCAT bus.

The battery pack uses four six-cell lithium polymer battery packs, each with a 5-Ah-rated capacity. The packs are connected in a two-serial two-parallel configuration, giving a nominal voltage of 44.4 V and a nominal capacity of 10 Ah. With 65 C-discharge-rate batteries, the pack is rated to deliver a peak current of 650 A.

A supervisory computer communicates with the robot computer through a Wi-Fi link, using a wireless router mounted on the robot. The supervisory computer, a laptop running MATLAB and Simulink on Windows 8.1, displays diagnostic information and is used to calibrate and enable the robot. Movement commands are generated by a PlayStation 3 controller connected to the supervisory computer and are then sent via the wireless link to the robot computer.

The robot uses an emergency stop (E-stop) system to disable the motor drivers and prevent damage to the robot or injury to the operators. An E-stop bus with ring topology allows stop signals or physical breaks in the bus to reliably propagate to everything in the chain. When the bus is pulled high, the motor drivers are enabled and are allowed to send current to the motors. When the pull-up is removed—because of a stop condition generated by the robot computer, the E-stop button being pressed, or a wire being severed—current to the motors is disabled, and the Medulla modules enter a stop state.

Control Algorithm Overview

The controllers used on ATRIAS are designed to work with the dynamic hardware. We used reduced order based on the spring-mass model and mechanical insights to develop behaviors rather than high-DoF model-based control. The behaviors do not require any preplanning, and the stability of the gait is not tied to the existence of disturbance models. Instead, the robot is purely reactive to the changing world.

Joint compliance relates forces to deflections, measurable with the high-accuracy joint encoders and allowing open-loop trajectories to interact with unexpected or nontrivial contact states. Knowing that forces will be exerted exactly opposite to contact disturbances, we can create controllers that are open-loop stable with respect to changes in the environment. In a way similar to hardware compliance, low gains for motor trajectory tracking allow the controller to loosely track discontinuous trajectories without inducing extreme accelerations.

Several simultaneous behaviors combine to create the overall behavior of the robot. Controllers blend together based on leg force rather than switching out distinct controllers for different phases of the gait. Figures 5–8 illustrate the concepts used in the control algorithm, including

- clock-based stepping
- velocity-based foot placement
- soft transitions between swing and stance
- torso balance
- energy injection against controlled damping.

These behaviors are in effect for both legs simultaneously, and the individual progressions are phase-shifted by the alternating clocks for each leg. A detailed look at the controller can be found in [5].

Clock-Based Stepping

Stepping is based on a clock cycle, where the frequency of steps matches the natural frequency of the spring-mass dynamics of the robot. In effect, the system as a whole acts similarly to a forced oscillator with dissipation, which entrains the robot to a dynamic oscillating gait [Figure 5(b)]. Stepping trajectories are parameterized by a stepping height (the apex of the step trajectory) and a nominal touchdown target, which is chosen by the foot placement behavior.

Figure 5 shows the correspondence between clock cycles and the interpolated trajectory of the toe. There is one clock

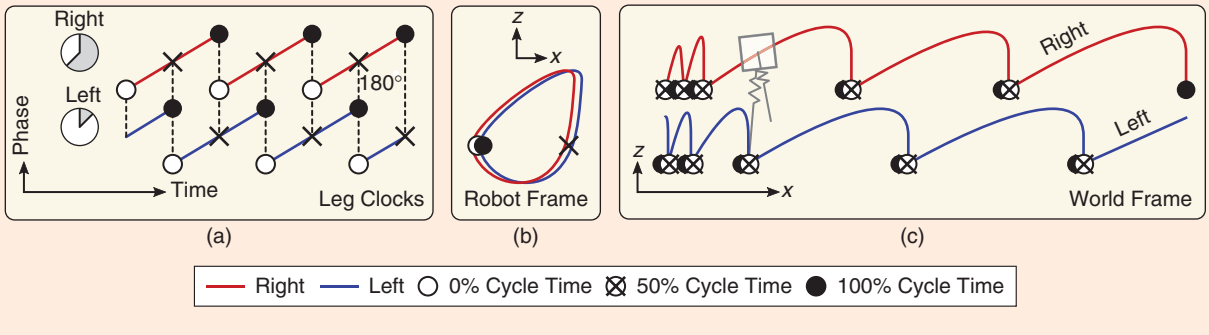

Figure 5. Trajectories for each leg and the correspondence between (a) two 180° out-of-phase clocks, which drive the leg motions. The clocks wrap from step to step and drive the periodic motions of the robot. Toe trajectories as (b) seen from the moving robot's frame and (c) they move through the world.

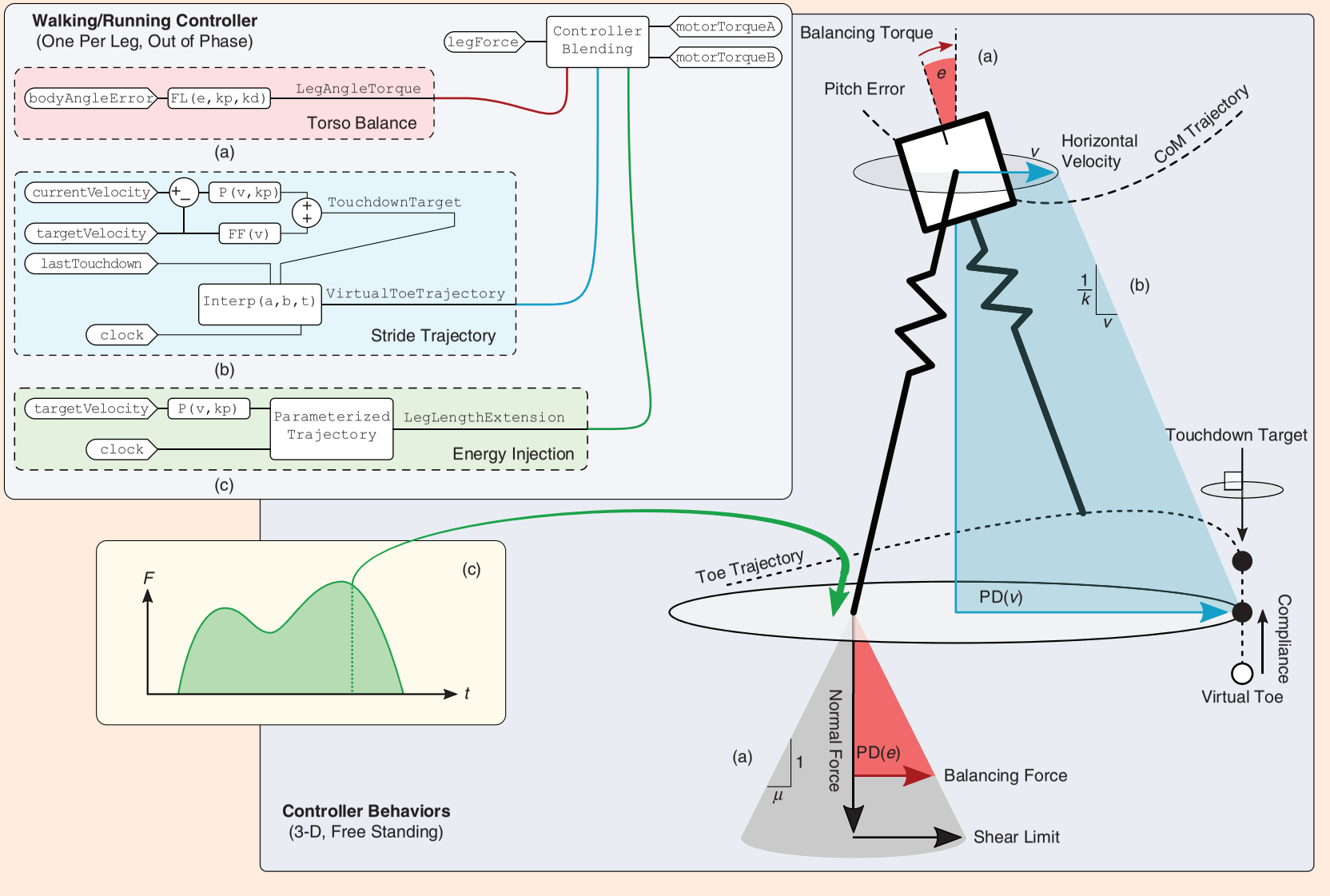

Figure 6. A high-level view of the three main behaviors of the control algorithm. (a) Torso balance attempts to keep the torso upright, applying restoring torques at the hip based on a feedback-linearization control law. Because each leg has both stance and aerial phases, the balance controller must be blended in and out as the contact force changes. The resulting shear force on the ground is always limited to be within an approximate friction cone. (b) Each stride trajectory has a target touchdown location for the toe, where the toe will be ground-speed matched and lowered toward the ground. This vertical descent continues even after the physical toe begins contact and the virtual toe is driven deeper into the ground, where the leg compliance can supply restoring forces. Vertical descent also improves the chances that a disturbance will affect the height of the contact only. The touchdown target location is a result of feed-forward processing of the current velocity adjusted by the difference between the current and target velocities. (c) Energy injection is parameterized as extra leg extension in the second half of the stance phase. Stepping and energy injection are both driven by an internal clock cyclically progressing through the phase [0,1].

for each leg, each 180° out of phase, and each periodically wrapping as the gait advances [Figure 5(a)]. One clock cycle corresponds to one step for its corresponding leg. The clock cycles drive most of the trajectory interpolation for the gait [Figure 5(c)], reliably sequencing controller events (as opposed to triggering based on intermittent events, such as toe strikes).

Stride Trajectory and Foot Placement

Footfalls are placed such that the robot's velocity gradually approaches the desired direction. The controller takes a directional influence from a human operator and attempts to move in that direction, but individual steps are not controlled by the operator.

Each step is calculated using a feed-forward model of toe placement based on the transverse velocity of the robot (removing the vertical component), as illustrated in Figure 6(b). The initial calculation would, ideally, carry the robot along its current path, if used repeatedly in a number of steps. The feed-forward model is augmented with proportional derivative (PD) control around the transverse velocity error in both the x (forward) and y (right) directions, which controls the acceleration and deceleration of the robot as new velocity commands are issued.

The continual stepping of the feet due to the clock cycle aids in controlling the velocity; no single footfall corrects the robot's velocity, and frequent stepping gives more opportunities to recover from disturbances. Disturbances and model errors will continually change the robot's velocity, so there is no reason to attempt to enforce deadbeat control; asymptotic control works very well in this case.

Touchdown Transitions

The virtual toe trajectory (the location of the toe for undeflected springs) is open-loop and continuous through stride and touchdown and into stance. The mechanism compliance allows for a smooth transition and gradual change in contact forces between the toe and the ground, which impact at nonzero velocity.

Open-loop transitions are an important feature of the controller and are deliberately crafted to be independent of contact sensing, because sensing the exact moment of touchdown is deceptively difficult to achieve in practice (switches bounce, force thresholds take time to reach, and either may be triggered accidentally). In dynamic environments, it is not even useful to know a particular instant of touchdown, because the foot may slide, break and make contact repeatedly (chatter), or sink into soft terrain.

One open-loop toe trajectory is continuous in the time before and after contact but is designed to decompose into two distinct controllers based on the real-world contact state. Stepping uses a ground-speed-matched trajectory where the toe vertically descends to the ground height at that point. This method does not require knowledge of exactly when the foot contacts the ground, and the same vertical trajectory is followed after the foot makes contact. Before touchdown, this trajectory corresponds to a ground-speed-matching behavior, but, after touchdown, the same trajectory continues to drive the foot into the ground, resulting in a nearly axial restorative force. This second behavior is the trivial stance controller for spring-mass robots, i.e., holding a constant leg length through stance and balancing the leg angle torques such that the contact force goes through the mass center of the robot.

Torso Balance

After toe contact is established, contact forces begin rising and expand the ability of the torso balance controller to apply hip torques against the ground. A friction cone approximation limits the balancing hip torques, preventing the toe from slipping on the ground, as illustrated in Figure 6(a). The torque is calculated for pitch and roll DoFs using a feedback-linearization law to force the torso upright [5]. The effect of this behavior is added to the nominal stance behavior of leg length forces.

Energy Injection and Damping

A large part of the robustness of the controller comes from the addition of controlled damping. The controller following the motor trajectory has PD gains tuned such that roughly half of the overall leg compliance comes from the motor and the other half from the passive springs. Having such soft gains makes the robot more compliant and removes energy through damping in the motors and transmission.

Energy injection replenishes the system's mechanical energy after some is removed by damping, disturbances, or elevation changes. Through the first half of stance, the leg length is nominally constant, remaining a passive spring. In the second half of stance, the leg begins extending to drive the robot forward. The amount of extension is proportional to the desired transverse velocity, as visually indicated in Figure 6(c).

The interplay of energy injection and damping has a stabilizing effect on the system. As a simple example, a vertical hopping robot can find an open-loop, stable hopping height by injecting a fixed amount of energy into each hop, while leg damping removes energy proportional to the touchdown velocity and stance duration; the energy injection will naturally balance the energy removal. Figure 7 shows how physical damping can close the loop on velocity control. Similarly, for the ATRIAS robot, periodic forcing in the forward direction (through leg extension in the second half of stance) finds a naturally stable speed when balanced by the damping in the legs.

Figure 8 shows how the impulses generated by disturbances decay as a result of damping and how periodic forcing drives the robot forward without needing to directly sense and regulate velocity. The average direction of the envelope in Figure 8 gives the net velocity of the robot. The controller needs to supply only periodic forcing during locomotion, and damping will remove the effect of extraneous impulses due to disturbances. Damping also removes part of

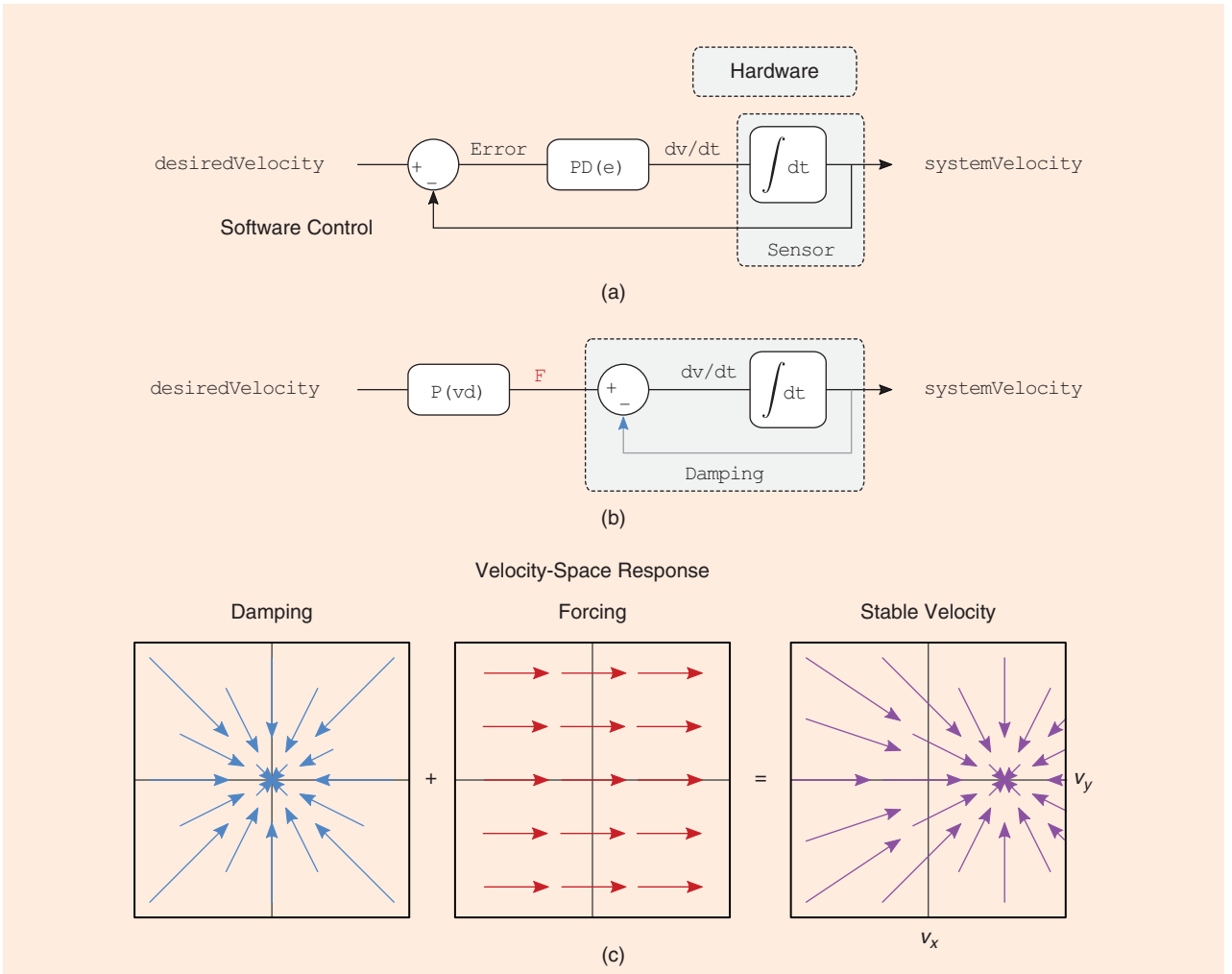

Figure 7. A simple example of open-loop velocity control by balancing directional forcing against isotropic damping. (a) Feedback control of velocity requires an accurate measurement of the system velocity. (b) Feed-forward forces combine with damping in the world to close the feedback loop for velocity, with the added benefit that accurate sensing of the ground-truth velocity is no longer necessary, nor is accurate application of force in response to changes in velocity. (c) In velocity space, where the current velocity of a system is represented by a point in that space, forces represent the gradual change in position of those points. The force of damping always acts toward the origin. If an external force is applied, the equilibrium velocity shifts in the direction of that force.

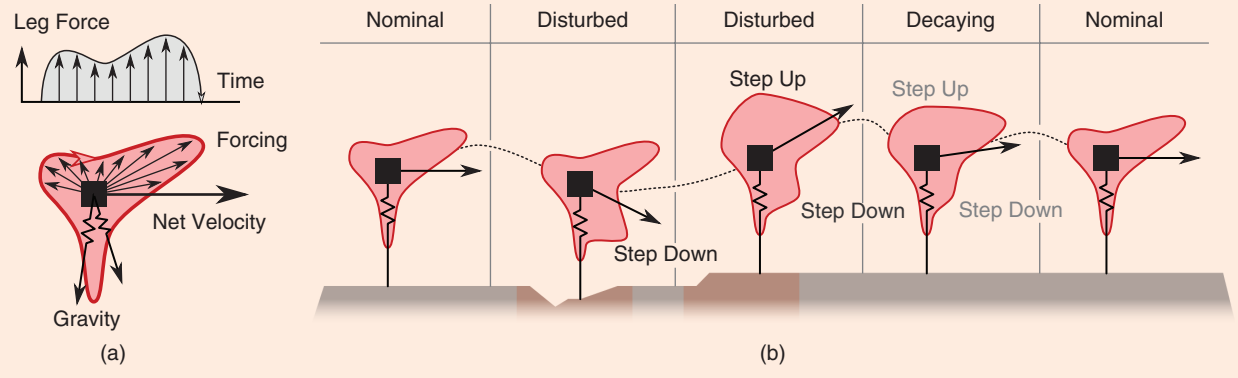

Figure 8. The effect of physical damping on the net velocity of the robot. (a) Envelopes around the mass center represent the history of directional impulses on the robot; impulses in the same direction sum, while (b) impulses in different directions push out the envelope in those directions. The envelopes record impulses only from forces other than damping, which is represented by the gradual decay of the envelope.

the effect of the periodic forcing, but that impulse is being continually injected, so it remains dominant. It is not necessary for the controller to sense and act on current velocity feedback; it must only supply feed-forward forcing in the desired direction.

Methods and Processes

Having such an atypical design and control paradigm for a humanoid, ATRIAS required interactive tuning and gradual addition of behaviors to add capabilities to the controller. A high-fidelity SimMechanics model made it easy to continually tune and adjust the controllers, with results that could be immediately used on the robot.

Tools

Having a quality software toolchain was vital for reaching the goal of a live show at the DARPA Robotics Challenge. A combination of off-the-shelf software and hardware components was selected and assembled to form a control system that required minimal maintenance effort. As an added benefit, the ATRIAS controller could be written as native MATLAB code. This toolchain allowed for rapid iteration of controllers and simple testing on the full-order robot.

A multibody simulation of the ATRIAS biped allowed for extremely efficient and worry-free testing of new control ideas [44]. Modeled in SimMechanics and controlled through Simulink, the simulation was a good approximation of the behavior of the real robot, down to the same controller interface. A controller could be tuned using the simulation and then required only minor adjustment when implemented on the robot. The porting process was handled almost entirely by the software, requiring only a flag indicating whether the controller was running in the simulation or on the hardware.

Our final controller occupied a concise 880 lines of MATLAB code, not including the Simulink architecture. This did not include microcontroller or low-level safety code, only the final control function that mapped the robot's state to motor commands.

Figure 9 shows the quality of the simulation, where the robot was kicked during a physical test and given the same impulse in simulation. The resulting robot trajectories were nearly identical, from the overall torso path down to the motion and timing of the leg movements.

Development of Behaviors and Capabilities

We started with an intuitive, bare-bones controller for two-dimensional (2-D) push-assisted walking on a spherical boom. Adding a rear leg push-off behavior allowed the robot to walk on its own. This process continued, adding behaviors to the simulation, tuning them, and applying them to the robot. Soon, we had a controller that could stably walk and run in 3-D through rough and unstable terrain. There were several significant stages in developing this controller, starting with a basic controller and incrementally adding hand-coded behaviors.

State-Based Push-to-Walk on Flat Ground: 2-D

The inaugural behavior was primitive stepping with a fixed stride length, designed simply to put one foot in front of the other. This behavior was not automatic, so an operator had to be present to push the robot forward from step to step. Stance leg and swing leg were determined by which physical leg was applying greater force to the ground, a parameter that typically switched when the hip was halfway between footfalls. Forces in the leg length and leg angle were measured by sensing the deflection of the two series springs in each leg.

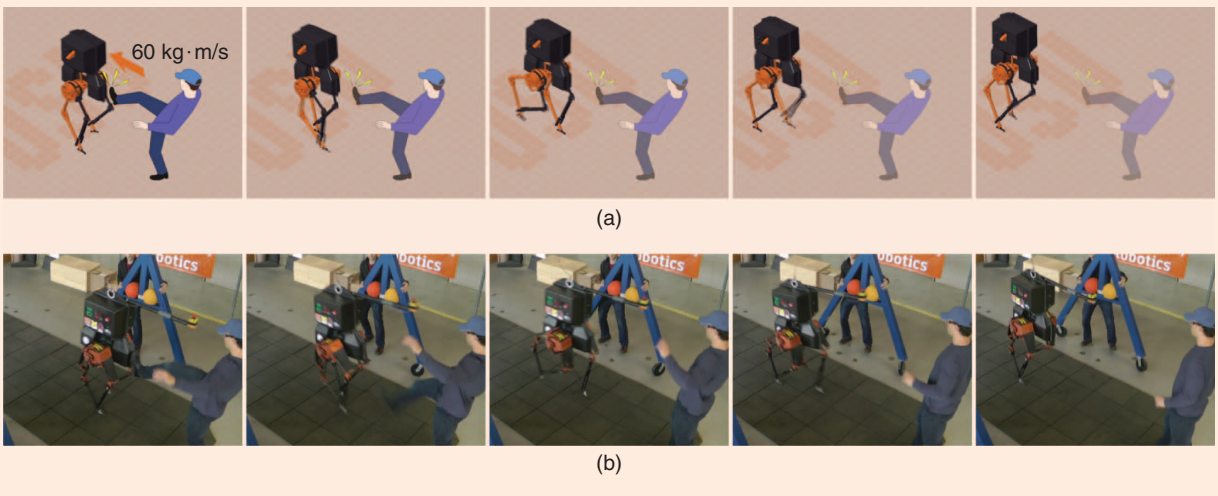

Figure 9. An example of the use of full-body simulation in the development of ATRIAS's control. (a) A film strip of the SimMechanics model of ATRIAS with a hardware controller being simulated with a large horizontal impulse (aesthetically illustrated with an overlaid kicking human). (b) Using the same controller, the physical robot is kicked to test its disturbance rejection. (Figure courtesy of Christian Hubicki.)

To take the next step, the foot of the leading leg was brought to a point above the next target and then lowered until it contacted the ground. The foot trajectory from the previous midstride to the next midstride was parameterized by the x-location of the hip between midstrides. After contact, the motors continued moving as if the foot was still in free space, causing the springs to deflect and apply a restorative force. Torso stabilization was achieved through PD-controlled hip torques on the legs, scaled by the vertical ground force of each foot (i.e., a scaled friction cone).

Self-Regulated Walking on Flat Ground

Incorporating a push-off behavior to the trailing leg allowed the robot to propel itself forward, adding back lost energy. Low proportional gains for the joint trajectories and high derivative gains damped energy out of the gait and stabilized the robot. The interaction between energy injection in the forward direction and energy removal by the joints led to a stable forward walking speed.

Stepping in Place: Incorporating a Clock-Driven Stepping Cycle

The previous behaviors were not self-starting, so we added a clock-driven stepping cycle. This meant the robot would always be in motion, even at zero forward velocity. It began by stepping in place, trying to maintain a fixed horizontal position. Footfalls were selected to remove any extraneous momentum by shifting the horizontal position of the step proportionately with velocity error.

Speed Changes, Forward, and Reverse

With the stepping behavior implemented, we began varying the forward velocity command from positive to zero, to negative, and back. The robot began by stepping in place at zero velocity and then slowly increased the forward speed to begin walking forward. The stride length was varied, depending on the forward speed. The push-off behavior was always in effect as a result of the clock-driven stepping cycle.

Numerous Obstacles and Stability Testing

At this point, the controller was able to robustly walk in moderate step-ups, step-downs, loose terrain, and slippery terrain in 2-D. It could also handle pushes and kicks that either accelerated or impeded its forward progress.

Stepping in Place: 3-D

The next big step in creating a controller for real-world locomotion was taking the robot off its support boom, which is the walking equivalent of removing the training wheels from a new cyclist's bike. Now, the robot had to control its lateral velocity and torso roll in addition to forward velocity and pitch. We modified the clock-based stepping controller to account for these additional DoFs rather than adding entirely new behaviors. The first test of this capability was simply stepping in place with a zero-velocity goal. At this point, we also made the strides fully dependent on the clock, removing any state-based feedback.

Robust Stepping, Obstacles, Kicks, and Dodgeballs

Stability is the most important factor for real-world locomotion, so we spent time making sure the stepping controller could handle large velocity changes and alterations in ground height and consistency. Our impulsive testing included small pushes, a dodgeball barrage, and heavy kicks. In separate tests, foam squares and wooden steps disrupted the flat-ground stepping cycle. The controller's behavior took the extraneous velocities from these disturbances and removed them in several steps, settling into a zero-velocity stepping pattern.

Having a quality software toolchain was vital for reaching the goal of a live show at the DARPA Robotics Challenge.

Directed Stepping

Just as stepping in place led to speed changes in 2-D, the 3-D stepping controller was given directional commands. A video game controller influenced the velocity of the robot by suggesting a direction of motion, which the robot tried to satisfy. The speed change was not immediate, but the velocity asymptotically approached the commanded speed and direction.

Robustness with Obstacles

We performed another round of robustness testing for the directional walking controller, this time in 3-D. We used more unstructured terrain, with foam pads, blocks, and plywood steps. At this point, we designed and built a lightweight mobile gantry that could be pushed around by a pair of researchers while a third drove the robot using the game controller.

Running on Flat Ground

Given enough space, the controller could pick up sufficient speed to enter an aerial phase. As there is no ground contact in flight, we could not judge the forward position of the robot through the stance leg. Instead, we gauged forward position by integrating the last known forward velocity. Because forward velocity in flight was constant and flight times were relatively small, this approach worked well for maintaining ground-speed-matched toes.

Locomotion Capabilities

We report ATRIAS's walking and running capabilities in terms of robustness (as measured by both terrain variation and external perturbations), speed, and energy economy. These capabilities were assessed in a variety of experimental tests in the lead-up to the DARPA Robotics Challenge.

Robustness

ATRIAS's robustness to complex terrain was tested on a variety of surfaces, uneven structures, and inclines. We conducted testing on nonrigid surfaces, such as grass, soft foam, and artificial field turf [Figure 10(a), (e), and (k)], [27], [49], [51]. Furthermore, we tested spontaneous transitions between surfaces to show robustness without any tuning of control parameters. Figure 10(b), [49] shows a snapshot of ATRIAS transitioning between walking on grass and pavement, and Figure 10(e) between soft foam and particle board. This

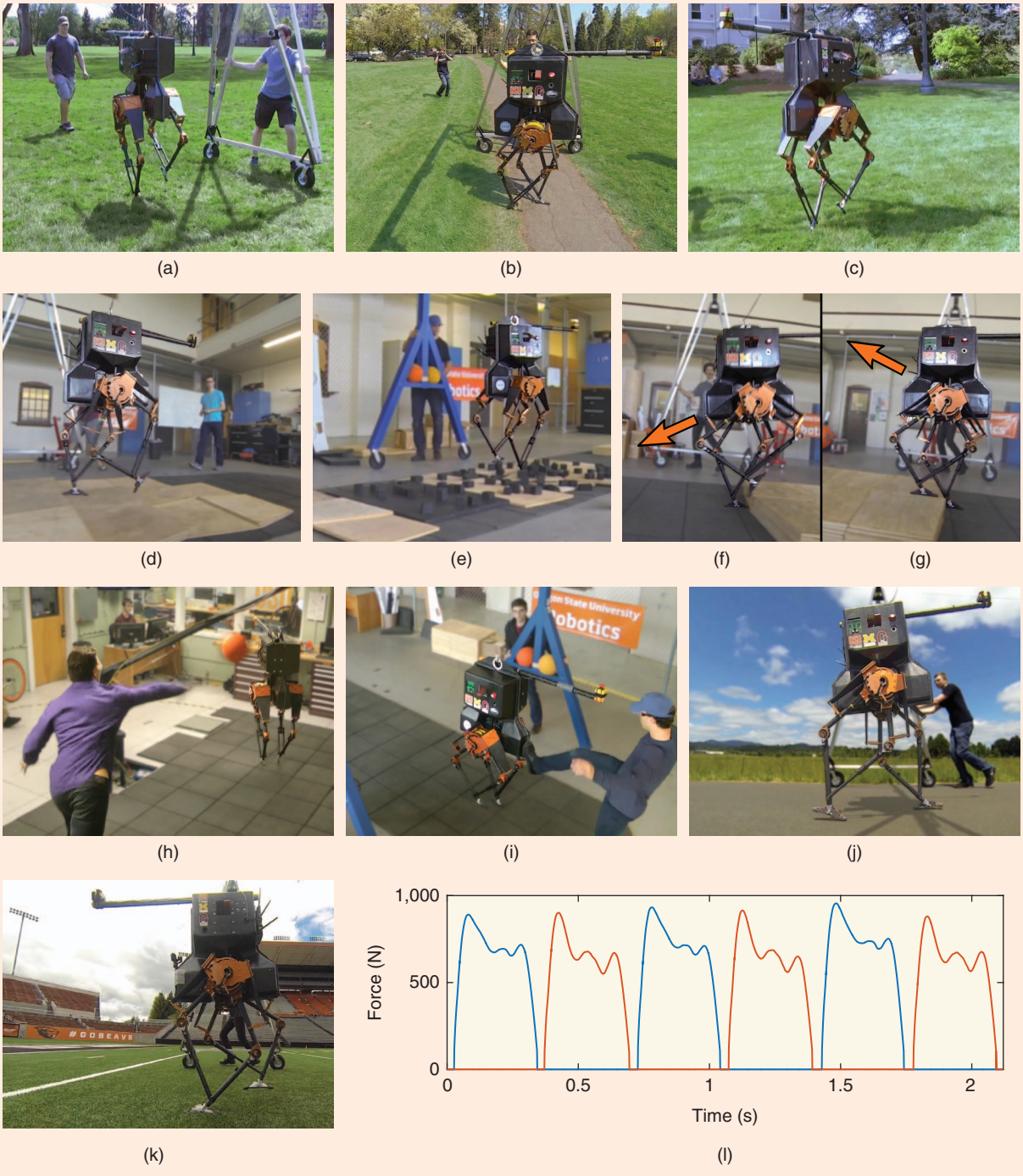

Figure 10. Various experiments with ATRIAS (a) walking on grass, (b) transitioning from pavement to grass, and (c) walking up a 15° grassy slope. In-lab obstacles, (d) transitions between wooden boards and soft foam, (e) randomly structured boards, and (f) stepping up and (g) stepping down a 15-cm platform, all of which were negotiated blindly. External disturbances included (h) repeated dodgeball strikes and (i) strong kicks. High-speed tests included (j) a top speed of 2.5 m/s and (k) a smooth transition from rest to walking to running and back to rest on stadium turf. (l) The plot for the vertical ground-reaction forces for each leg, with gaps between indicating short periods of flight. (Figures courtesy of Christian Hubicki and Patrick Clary.)

performance suggests that ATRIAS can walk stably without significant sensitivity to surface dynamics.

For our demonstration, we aimed to show locomotion on rough ground without any vision or prior planning. To create uneven ground in the laboratory, we tested walking on various arrangements of stacks of plywood. Figure 10(d) [50] shows the robot walking quickly (1.8 m/s) on a randomly structured obstacle (maximum height 9.5 cm), coming to a controlled stop at the end of the structure. The most extreme laboratory obstacle tested was a 15-cm-tall platform. In 11 consecutive tests, the robot successfully stepped onto this platform, walked a few elevated steps, and stepped off [shown in Figure 10(f) and (g)], [52]. Because the robot was unable to plan for the obstacle, some of the foot placements were not clean, including one test where the robot landed on the obstacle on the point of its toe. The control algorithm was able to recover in spite of these unexpected contact modes and timings. Furthermore, in an outdoor test, the robot was able to walk up and down a 15° slope [Figure 10(c)], [49].

We also tested ATRIAS's response to unexpected disturbances, such as repeated dodgeball strikes [Figure 10(h)], [53]. To deliver a much larger test impulse to a human-sized robot, we gave the torso a series of firm kicks [Figure 10(i)], [54]. When stepping in place, the robot was able to recover from kicks imparting 60 kg·m/s of momentum without falling. (The size of the impulse delivered was inferred from simulating impulse disturbances in the high-fidelity simulator.) This impulse is the equivalent of instantaneously accelerating the robot to 1 m/s.

Speed

ATRIAS was able to match commanded speeds between zero and 2.5 m/s and performed similarly well in both the forward and reverse directions, though we noted that the robot had the ability to achieve slightly higher speeds in the leftward direction as depicted in Figure 10(j) [55]. The latter figure shows a photo of ATRIAS reaching its top speed of 2.5 m/s (9 km/h) in an outdoor test on an asphalt path. After accelerating faster than 2.0 m/s, short aerial periods with no ground contact emerged, resulting in a transition to a running gait. This ability to transition between walking and running gaits was accomplished without switching between controller structures. Figure 10(k) shows a snapshot of ATRIAS after a transition to running during an outdoor test on artificial field turf, and Figure 10(l) illustrates the corresponding ground-reaction forces measuring the length of the aerial phases (an average flight time of 30 ms). This test also demonstrated the robot's ability to accelerate from rest to a run, and then to execute a controlled stop.

Energy Economy

We measured ATRIAS's energetic properties using two metrics: its operation time on a single battery charge and the mechanical and TCoT [15]. To test battery life, we commanded ATRIAS to step repeatedly in place until the battery pack was drained. The 48-V 10-Ah battery pack was drained in approximately 30 min of operation.

The TCoT is a nondimensional measure of the energy required to move a unit distance. The mechanical costs of transport (MCoT) accounts for only the mechanical energy being delivered by the actuators. The TCoT includes not just the mechanical cost to locomote, but the resistive losses in the electric motors and the onboard electronics overhead (including wireless communication and the control computer). We calculated the TCoT and MCoT for a 1.6-m/s walking test of ATRIAS. On average, the TCoT was 1.3, as measured at the battery pack (current and voltage). This is an improvement compared to the humanoid ASIMO's estimated TCoT of 3.2 [22] but is still far from the TCoT of 0.19 reported for the Cornell Ranger [16]. The average MCoT is 0.96, as measured at the actuator outputs (torque and speed).

Discussion of Controller Behaviors

The broad effects of the three controller components (torso balance, stride trajectory, and energy injection) can be seen rather intuitively in the resulting behavior of the robot. In the instance of directed perturbations, such as kicks and dodgeballs [Figure 10(h) and (i)], the stride trajectory control was the most visible. The sudden velocity change from the kick produced a significant velocity error, effectively commanding a large recovery step. The imposed time limitations between touchdown events in the stride generation ensured that a new foothold would be taken before the robot tipped too far. The effect of the torso balance control was somewhat less overt to the naked eye but was also most clear during the kicking experiment. After the initial perturbation and near the transition between the recovery steps, the torso began to tip. However, once a new foothold was secured, the torso snapped back to its vertical position quite quickly.

The energy injection behaviors were most pronounced in large [Figure 10(f) and (g)] or sustained terrain changes [such as the hill climbing in Figure 10(c)] and when achieving fast running speeds [Figure 10(j) and (k)]. After stepping on a tall obstacle, significant velocity was lost, which registered as a need to inject more energy and push up onto the obstacle. When walking uphill, this additional push-off persisted and added the gravitational potential energy necessary to continue upward (and the reverse was true when descending). Furthermore, when commanded to move sufficiently fast, enough energy was injected through push-off so that the robot left the ground. In essence, running manifested not as a distinctly programed behavior, but as a necessary consequence of injecting enough energy to locomote faster.

We also emphasize that the blending of the controllers was critical to achieving the reported results. The smoothed transitions from stance to nonstance control were likely helpful in randomly uneven [Figure 10(d) and (e)] or soft terrain [Figure 10(a), (b), and (k)]. By using force as a smooth criterion for switching, the switch to stance was dependent on a firm foothold being achieved. This meant that torso-balancing

ground torques and energy-injecting push-offs would be delayed on soft ground or an unexpected drop and rushed when landing on higher ground or stubbing its toe. This change in timing prevented the controller from applying large ground forces when they were not feasible.

Verification of Compliant Dynamics

We further sought validation that the designed passive compliance was actually significant when exhibiting these locomotion capabilities. Specifically, we asked whether the springs were deflecting enough, such that they had an appreciable effect on the gait dynamics during typical locomotion. Figure 11 plots the passive spring deflection for each leg's length (data collected during the same 1.6-m/s walking experiment used to calculate the TCoT in the "Energy Economy" section). The peak leg deflection during walking was approximately 5 cm of the 85-cm leg length. In terms of energetics, computing the energy stored in each of the leg mechanisms' two component springs corresponded to approximately 20–25 J peak per leg, which roughly equated to the kinetic energy of the 60-kg robot traveling at 0.81–0.91 m/s. Evidently, then, passive compliance is integral to ATRIAS's dynamics.

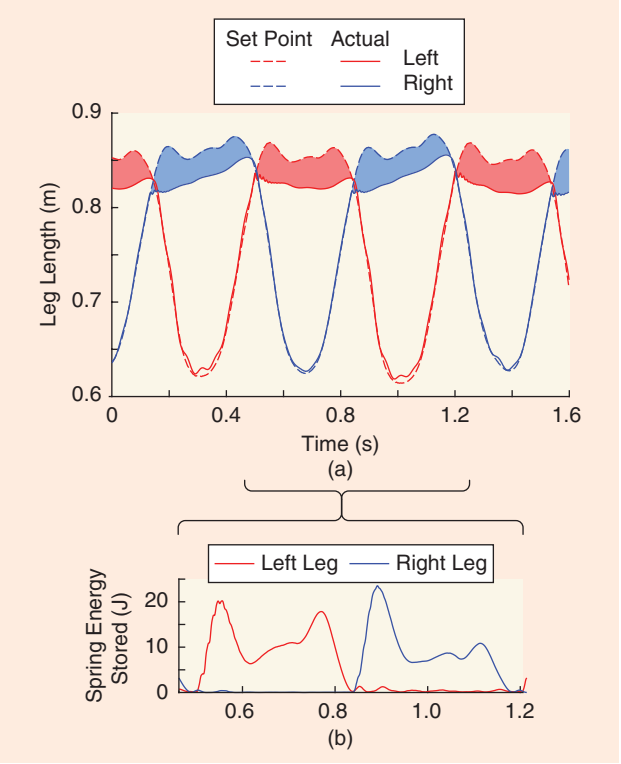

Figure 11. A verification that passive compliance plays a significant role in the dynamics of a walking gait. (a) A plot of the set point of the leg length, the length as measured by the actuator position compared with the actual measured leg length, which includes spring deflection. The shaded regions indicate the passive deflection of the leg when in contact with the ground. (b) A plot of the energy stored in the springs, which peaks between 20 and 25 J in each leg. This equates to the kinetic energy of the 60-kg ATRIAS traveling at 0.81–0.91 m/s.

This degree of deflection and energetic relevance is important for distinguishing this passive compliance approach from the more general class of series-elastic actuation. Series-elastic actuation is often used for force measurement (enabling impedance control techniques), for which comparatively stiff springs are a satisfactory solution. However, as the springs become very stiff, the compliance itself becomes less relevant to the dynamics of the gait. When the time scales of spring compression are orders of magnitude shorter than the time scales of the gait cycle, the compliant dynamics can be decoupled from the dynamics and control of a robot's overall motion. Computing the energy stored in the springs is a good indicator of whether the compliance is significant to the gait dynamics, because stored energy approaches zero with increasing stiffness.

Demonstration at the DARPA Robotics Challenge

In the course of two days at the beginning of June 2015, ATRIAS had seven successful shows in front of live audiences in Pomona, California. Each show demonstrated walking on rough terrain, running on flat ground, kicks, and dodgeball impacts. Not once did ATRIAS crash or fall during these demonstrations. We performed four shows beside our tent within the Expo area and three in front of the Fairplex Grandstands, where the main event was taking place.

Lessons Learned

The ATRIAS biped pushes template matching to the extreme in its aim to embody the SLIP model. It has carbon-fiber legs so light they are fairly fragile and require mechanical overload protection. Even at this end of the scale of passive dynamics, there are enough discrepancies between the reduced-order SLIP model and the robot to cause issues for model-based controllers. In the end, SLIP-inspired controllers were mixed with natural intuitions and tested in a multibody simulation to achieve our results.

Practical Control Development

Design Controllers Based on Reduced-Order Insights, but Test with Multibody Simulators

During early development, we would select touchdown leg angles for the full-order robot to try to affect a particular apex height and forward velocity for a SLIP model. A lot of effort was put into deadbeat controllers to move between apex states. An equal amount of effort was put into ground-reaction force controllers and virtual-pivot-point controllers. As we found, these controllers were very sensitive to exact foot placement (centimeter variations would cause trouble) or to imprecise force vector control.

No robot will ever perfectly match a reduced-order model (at least not while matter still has mass), but it is easy for a robot to approximate simple spring-mass dynamics. The SLIP model was used extensively to inspire our controller, but that is where the relationship ends. We manually tuned our controller in our multibody simulation environment, finding natural frequency, stride-velocity proportionality, and other

parameters that worked for the full-order and heavily nonlinear system.

Exploit Rapid Iteration

The key to developing a working product, both hardware and software, is a quick design–test–evaluate cycle. Incremental testing allowed us to quickly go over ideas, discover what worked, and cut fruitless branches out of our search.

Allow for Adjustable Control Parameters

Shifting model parameters are a fact of life in robotics. Not only does ATRIAS wear and age like any robot, it can also behave slightly differently with every test. Trimming controls like those for a radio-controlled airplane helped balance the robot on different terrain, with slightly different link lengths due to manufacturing, and different amounts of onboard weight. These tuning parameters were built into the controller and could be adjusted on the fly.

Be Careful Not to Actively Control Any Behavior That Is Actually a Symptom of a More Subtle Control Target

This difficulty occurs frequently in the field of bipedal locomotion, i.e., the most important feature of a gait appears to be the center-of-mass (CoM) motion or ground-reaction forces, so many robots try to control exactly those. For highly underactuated and dynamic robots, controlling around a trajectory is extremely difficult; the control authority of the robot is limited and phase dependent. Simply by choosing a different control target, e.g., stride length, angular momentum, or vertical impulse, periodic CoM motions emerge naturally. Simple control targets generally require no preplanning and are reactive to changes in the environment, but they still excite the natural walking dynamics of the robot.

Moving Forward: Future Iterations

ATRIAS can walk and run at various speeds and on varied terrain, but has incredible difficulty standing still. The robot has a minuscule polygon of support, and active stabilization tests suggested just a tiny region of stability, even in simulation. (Investigations into using linear quadratic regulators to locally stabilize a fixed point associated with standing yielded an impractically small basin of attraction.) While ATRIAS can hold its position by stepping in place, this is not an energetically practical solution for idling. In future designs, having an ability to apply even limited stabilizing torques about the foot, while not impeding gait dynamics, would be helpful for stationary balancing, climbing stairs, and precise balancing between steps.

Turning is a major component of locomotion, but ATRIAS can only sidestep. Animals are able to zigzag and bank between obstacles and points of interest, and we want future robots to have that same ability. To do this, ATRIAS would need an extra actuator to control the long-axis rotation of the leg, applying yaw torques to the ground and turning the robot. Currently, the robot requires the human operator to manually steer via a carbon tube extending from its torso, and turning the robot breaks static friction between the feet and the ground.

Practical robots will need to be self-starting and self-parking. ATRIAS must be started from a hanging position, and the shutdown process effectively stops the robot in midair and causes it to fall. Future iterations should be able to stand alone from a parked position and return to that position when shut down.

Escalating emergency states could gracefully handle small errors without a full E-stop. Currently, there is only one E-stop case: shut down all motor drivers, crashing the robot. This case is triggered for everything from overheating motors and limit-switch triggers to a dangerous controller failure. We disabled many of these safeties for the live shows at the DARPA Robotics Challenge to prevent unnecessary halts.

Efficiency can continue being increased. ATRIAS uses Harmonic Drive gearheads for their small package, but they are extremely inefficient. In addition, an internal power loop, where one motor acts as a brake, unnecessarily dissipates energy. Leg design must analyze the task force and speed requirements as they relate to the mechanism kinematics, minimizing the work lost to self-braking [3], [25].

The real world is a chaotic and dangerous place for robots, but machines with increased autonomy will need to be able to withstand and recover from crashes. ATRIAS requires a safety tether to prevent it from falling, because it was designed to be a scientific demonstrator of spring-mass locomotion, not a durable field-ready product. Future robots should be sturdy enough to fall or to crash into trees.

Conclusions

The ATRIAS robot, with a combination of deliberately engineered passive dynamics and complementary control algorithms, was able to walk and run, without external power or support, in front of a live audience at the DARPA Robotics Challenge. In producing this live performance, ATRIAS demonstrated 2.5-m/s running, variable speed control, and the ability to recover from strong human kicks. Furthermore, the robot was able to traverse varied surface dynamics and obstacles as high as 15 cm without any planning or vision. To the best of our knowledge, this degree of terrain robustness has not been reported for a self-contained bipedal machine. What ultimately allowed for sufficiently fast progress was a commitment to rapid control iteration on hardware. However, by the nature of its highly compliant and underactuated design, every step along the way required ATRIAS to embrace its passive dynamics to keep moving forward.

Acknowledgments

This work was funded by the DARPA Maximum Mobility and Manipulation Program, Grants W31P4Q-13-C-0099 and W91CRB-11-1-0002; Human Frontier Science Program, Grant RGY0062/2010; and the National Science Foundation, Grant CMMI-1100232.

References

[1] M. H. Raibert, *Legged Robots That Balance*. Cambridge, MA: MIT Press, 1986.

[2] T. McGeer, "Passive dynamic walking," *Int. J. Robotics Res.*, vol. 9, no. 2, pp. 62–82, 1990.

[3] C. Hubicki, J. Grimes, M. Jones, D. Renjewski, A. Spröwitz, A. Abate, and J. Hurst, "ATRIAS: Design and validation of a tether-free 3D-capable spring-mass bipedal robot," *Int. J. Robotics Res.*, vol. 35, no. 12, pp. 1497–1521, 2016.

[4] M. Spong, "Underactuated mechanical systems," in *Control Problems in Robotics and Automation*, B. Siciliano and K. Valavanis, Eds. Berlin: Springer-Verlag, 1998, pp. 135–150. doi: org/10.1007/BFb0015081.

[5] S. Rezazadeh, C. M. Hubicki, M. Jones, A. Peekema, J. Van Why, A. Abate, and J. Hurst, "Spring-mass walking with ATRIAS in 3D: Robust gait control spanning zero to 4.3 kph on a heavily underactuated bipedal robot," in *Proc. ASME Dynamic Systems Control Conf. (ASME/DSCC 2015)*, 2015, pp. V001T04A003.

[6] M. Vukobratovic and B. Borovac, "Zero-moment point: Thirty five years of its life," *Int. J. Humanoid Robotics*, vol. 1, no. 1, pp. 157–173, 2004.

[7] Y. Sakagami, R. Watanabe, C. Aoyama, S. Matsunaga, N. Higaki, and K. Fujimura, "The intelligent ASIMO: System overview and integration," in *Proc. IEEE/RSJ Int. Conf. Intelligent Robots Systems*, Lausanne, Switzerland, 2002, pp. 2478–2483.

[8] I. W. Park, J. Y. Kim, J. Lee, and J. H. Oh, "Online free walking trajectory generation for biped humanoid robot KHR-3(HUBO)," in *Proc. IEEE Int. Conf. Robotics Automation*, 2006, pp. 1231–1236. doi: 10.1109/ROBOT. 2006.1641877.

[9] S. Kajita, F. Kanehiro, K. Kaneko, K. Fujiwara, K. Harada, K. Yokoi, and H. Hirukawa, "Biped walking pattern generation by using preview control of zero-moment point," in *Proc. IEEE Int. Conf. Robotics Automation (ICRA '03)*, 2003, pp. 1620–1626.

[10] S. Kuindersma, R. Deits, M. Fallon, A. Valenzuela, H. Dai, F. Permenter, T. Koolen, P. Marion, and R. Tedrake, "Optimization-based locomotion planning, estimation, and control design for the Atlas humanoid robot," *Autonomous Robots*, vol. 40, no. 3, pp. 429–455, 2015. doi: 10.1007/s10514-015-9479-3.

[11] R. Blickhan, "The spring mass model for running and hopping," *J. Biomech.*, vol. 22, no. 11–12, pp. 1217–1227, 1989.

[12] J. Schmitt and J. Clark, "Modeling posture-dependent leg actuation in sagittal plane locomotion," *Bioinspiration Biomimetics*, vol. 4, no. 4, Nov. 2009. doi: 10.1088/1748-3182/4/4/046005.

[13] M. Ernst, H. Geyer, and R. Blickhan, "Extension and customization of self-stability control in compliant legged systems," *Bioinspiration Biomimetics*, vol. 7, no. 4, Dec. 2012. doi: 10.1088/1748-3182/7/4/046002.

[14] M. Ahmadi and M. Buehler, "Controlled passive dynamic running experiments with the ARL-Monopod II," *IEEE Trans. Robot.*, vol. 22, no. 5, pp. 974–986, 2006.

[15] S. H. Collins, A. Ruina, R. Tedrake, and M. Wisse, "Efficient bipedal robots based on passive-dynamic walkers," *Science*, vol. 307, no. 5712, pp. 1082–1085, 2005. doi: 10.1126/science.1107799.

[16] P. A. Bhounsule, J. Cortell, A. Grewal, B. Hendriksen, J. G. Daniël Karssen, C. Paul, and A. Ruina, "Low-bandwidth reflex-based control for lower power walking: 65 km on a single battery charge," *Int. J. Robotics Res.*, vol. 33, no. 10, pp. 1305–1321, 2014. doi: 10.1177/0278364914527485.

[17] K. Sreenath, H-W. Park, I. Poulakakis, and J. W. Grizzle, "A compliant hybrid zero dynamics controller for stable, efficient and fast bipedal walking on MABEL," *Int. J. Robotics Res.*, vol. 30, no. 9, pp. 1170–1193, 2011.

[18] A. Hereid, S. Kolathaya, M. S. Jones, J. Van Why, J. W. Hurst, and A. D. Ames, "Dynamic multi-domain bipedal walking with ATRIAS through SLIP based human-inspired control," in *Hybrid Systems: Computation and Control*, M. Fráänzle and J. Lygeros, Eds. Berlin: ACM, 2014, pp. 263–272.

[19] A. E. Martin, D. C. Post, and J. P. Schmiedeler, "Design and experimental implementation of a hybrid zero dynamics-based controller for planar bipeds with curved feet," *Int. J. Robotics Res.*, vol. 33, no. 7, pp. 988–1005, 2014. doi: 10.1177/0278364914522141.

[20] M. Johnson, B. Shrewsbury, S. Bertrand, T. Wu, D. Duran, M. Floyd, P. Abeles, D. Stephen, N. Mertins, A. Lesman, J. Carff, W. Rifenburgh, P. Kaveti, W. Straatman, J. Smith, M. Griffioen, B. Layton, T. de Boer, T. Koolen, P. Neuhaus, and J. Pratt, "Team IHMC's lessons learned from the DARPA Robotics Challenge trials," *J. Field Robotics*, vol. 32, no. 2, pp. 192–208, Mar. 2015. doi: 10.1002/rob.21571.

[21] T. Erez, K. Lowrey, Y. Tassa, and V. Kumar, "An integrated system for real-time model predictive control of humanoid robots," in *IEEE/RAS Int. Conf. Humanoid Robots*, 2013, pp. 292–299.

[22] K. Kaneko, F. Kanehiro, M. Morisawa, K. Miura, S. Nakaoka, and S. Kajita, "Cybernetic human HRP-4C," in *Proc. 9th IEEE-RAS Int. Conf. Humanoid Robots*, Dec. 2009, pp. 7–14. doi: 10.1109/ICHR. 2009 .5379537.

[23] A. M. Abate, "Preserving the planar dynamics of a compliant bipedal robot with a yaw-stabilizing foot design," H.B.S. thesis, Mech. Eng., Oregon State Univ., Corvallis, OR, 2014.

[24] R. Blickhan, A. Seyfarth, H. Geyer, S. Grimmer, H. Wagner, and M. Günther, "Intelligence by mechanics," *Philos. Trans. Royal Soc. A: Math., Phys. Eng. Sci.*, vol. 365, no. 1850, pp. 199–220, Jan. 2007. doi: 10.1098/rsta.2006.1911.

[25] A. Abate, R. L. Hatton, and J. Hurst, "Passive-dynamic leg design for agile robots," in *Proc. IEEE Int. Conf. Robotics Automation (ICRA)*, 2015, pp. 4519–4524.

[26] M. A. Daley and A. A. Biewener, "Running over rough terrain reveals limb control for intrinsic stability," in *Proc. Nat. Acad. Sci. USA*, vol. 103, no. 42, pp. 15,681–15,686, Oct. 2006. doi: 10.1073/pnas.0601473103.

[27] Dynamic Robotics Laboratory. (2015, June 2). ATRIAS robot: Runs to the end zone. [Online]. Available: https://youtu.be/KeSkAPYAJc4

[28] S. Feng, E. Whitman, X. Xinjilefu, and C. G. Atkeson, "Optimization-based full body control for the DARPA Robotics Challenge," *J. Field Robotics*, vol. 32, no. 2, pp. 293–312, Mar. 2015. doi: 10.1002/rob.21559.

[29] C. T. Moritz and C. T. Farley, "Passive dynamics change leg mechanics for an unexpected surface during human hopping," *J. Appl. Physiol.*, vol. 97, no. 4, pp. 1313–1322, Oct. 2004. doi: 10.1152/japplphysiol .00393.2004.

[30] H. R. Vejdani, A. Wu, H. Geyer, and J. Hurst, "Touch-down angle control for spring-mass walking," in *IEEE Int. Conf. Robotics Automation (ICRA)*, 2015, pp, 5101–5106.

[31] H. W. Park, K. Sreenath, A. Ramezani, and J. W. Grizzle, "Switching control design for accommodating large step-down disturbances in bipedal robot walking," in *IEEE/RSJ Int. Conf. Robotics Automation (ICRA)*, May 2012, pp. 45–50. doi: 10.1109/ICRA.2012.6225056.

[32] R. J. Full and D. E. Koditschek, "Templates and anchors: Neuromechanical hypotheses of legged locomotion on land," *J. Experiment. Biol.*, vol. 202, no. 23, pp. 3325–3332, Dec. 1999.

[33] R. Pfeifer, F. Iida, and G. Gómez, "Morphological computation for adaptive behavior and cognition," *Int. Congr. Series*, vol. 1291, pp. 22–29, June 2006. doi: 10. 1016/j.ics.2005.12.080.
[34] H. Geyer, A. Seyfarth, and R. Blickhan, "Compliant leg behaviour explains basic dynamics of walking and running," in *Proc. R. Soc. Lond. B*, vol. 273, no. 1603, pp. 2861–2867, Nov. 2006. doi: 10.1098/rspb.2006.3637.
[35] D. L. Jindrich and R. J. Full, "Dynamic stabilization of rapid hexapedal locomotion," *J. Experiment. Biol.*, vol. 205, no. 18, pp. 2803–2823, Sept. 2002.
[36] B. G. Buss, A. Ramezani, K. Akbari Hamed, K. S. Griffin, B. A. Galloway, and J. W. Grizzle. "Preliminary walking experiments with underactuated 3D bipedal robot MARLO," in *Proc. IEEE Int. Conf. Intelligent Robots Systems (IROS 2014)*, 2014, pp. 2529–2536.
[37] S. H. Collins and A. Ruina, "A bipedal walking robot with efficient and human-like gait," in *IEEE Conf. Robotics Automation*, Apr. 2005, pp. 1983–1988.
[38] W. J. Schwind, "Spring loaded inverted pendulum running: A plant model," Ph.D. dissertation, Dept. Elect. Eng., Univ. Michigan, Ann Arbor, MI, 1998.
[39] A. Seyfarth, H. Geyer, and H. M. Herr, "Swing-leg retraction: A simple control model for stable running," *J. Experiment. Biol.*, vol. 206, no. 15, pp. 2547–2555, Aug. 2003. doi: 10.1242/jeb.00463.
[40] S. Kohlbrecher, A. Romay, A. Stumpf, A. Gupta, O. von Stryk, F. Bacim, D. A. Bowman, A. Goins, R. Balasubramanian, and D. C. Conner, "Human-robot teaming for rescue missions: Team ViGIR's approach to the 2013 DARPA Robotics Challenge trials," *J. Field Robotics*, vol. 32, no. 3, pp. 352–377, May 2015. doi: 10.1002/rob. 21558.
[41] M. W. Spong, "Partial feedback linearization of underactuated mechanical systems," in *IEEE/RSJ Int. Conf. Intelligent Robots Systems*, Munich, Germany, Sept. 1994, pp. 314–321.
[42] K. Sreenath, H.-W. Park, I. Poulakakis, and J. Grizzle, "Embedding active force control within the compliant hybrid zero dynamics to achieve stable, fast running on MABEL," *Int. J. Robotics Res.*, vol. 32, no. 3, pp. 324–345, Mar. 2013. doi: 10.1177/0278364912473344.
[43] I. R. Manchester, U. Mettin, F. Iida, and R. Tedrake, "Stable dynamic walking over uneven terrain," *Int. J. Robotics Res.*, vol. 30, no. 3, pp. 265–279, Jan. 2011. doi: 10.1177/0278364910395339.
[44] W. C. Martin, A. Wu, and H. Geyer, "Robust spring mass model running for a physical bipedal robot," in *Proc. IEEE Int. Conf. Robotics and Automation (ICRA)*, 2015, pp. 6307–6312.
[45] P. M. Wensing and D. E. Orin, "High-speed humanoid running through control with a 3D-SLIP model," in *Proc. IEEE/RSJ Int. Conf. Intelligent Robots Systems (IROS)*, Nov. 2013, pp. 5134–5140. doi: 10.1109/IROS.2013.6697099.
[46] E. Westervelt, J. W. Grizzle, and D. E. Koditschek, "Hybrid zero dynamics of planar biped walkers," *IEEE Trans. Autom. Control*, vol. 48, no. 1, pp. 42–56, Jan. 2003.
[47] S.-J. Yi, S. G. McGill, L. Vadakedathu, Q. He, I. Ha, J. Han, H. Song, M. Rouleau, B.-T. Zhang, D. Hong, M. Yim, and D. D. Lee, "Team THOR's entry in the DARPA Robotics Challenge trials 2013," *J. Field Robotics*, vol. 32, no. 3, pp. 315–335, May 2015. doi: 10.1002/rob.21555.
[48] M. Zucker, S. Joo, M. X. Grey, C. Rasmussen, E. Huang, M. Stilman, and A. Bobick, "A general-purpose system for teleoperation of the DRC-HUBO humanoid robot," *J. Field Robotics*, vol. 32, no. 3, pp. 336–351, May 2015. doi: 10.1002/rob.21570.
[49] Dynamic Robotics Laboratory. (2015, Apr. 27). ATRIAS bipedal robot: Takes a walk in the park. [Online]. Available: https://youtu.be/dl7KUUVHC-M
[50] Dynamic Robotics Laboratory. (2015, June 3). ATRIAS robot: Traverses rough terrain at 6.6 kph (4.1 mph). [Online]. Available: https://youtu.be/VBDysRlrfcY
[51] Dynamic Robotics Laboratory. (2015, Apr. 9). ATRIAS robot: Tackles an obstacle course. [Online]. Available: https://youtu.be/1CfHbBAv6vo
[52] Dynamic Robotics Laboratory. (2015, June 1). ATRIAS robot: Climbs a 15-cm obstacle. [Online]. Available: https://youtu.be/dOoQTPqnLqI
[53] Dynamic Robotics Laboratory. (2015, Apr. 22). ATRIAS robot: Getting kicked – robot vs. simulation. [Online]. Available: https://youtu.be/yYvrTc3-uVU
[54] Dynamic Robotics Laboratory. (2015, June 1). ATRIAS robot: Dodgeball barrage. [Online]. Available: https://youtu.be/K1m8fYsPMnY
[55] Dynamic Robotics Laboratory. (2015, June 4). ATRIAS robot: 9.1 kps running speed (5.7 mph). [Online]. Available: https://youtu.be/U4eBRPHYCdA

Christian Hubicki, Georgia Institute of Technology, Atlanta, United States. E-mail: christian.hubicki@gmail.com.

Andy Abate, Oregon State University, Corvallis, United States. E-mail: abatea@onid.oregonstate.edu.

Patrick Clary, Oregon State University, Corvallis, United States. E-mail: claryp@oregonstate.edu.

Siavash Rezazadeh, University of Texas at Dallas, United States. E-mail: s.rezazadeh@gmail.com.

Mikhail Jones, Agility Robotics, Albany, Oregon, United States. E-mail: jonesmik@engr.orst.edu.

Andrew Peekema, Honeybee Robotics, New York, United States. E-mail: peekemaa@onid.orst.edu.

Johnathan Van Why, Alphabet Inc., Mountain View, California, United States. E-mail: vanwhyj@onid.orst.edu.

Ryan Domres, Oregon State University, Corvallis, United States. E-mail: ryan.domres@gmail.com.

Albert Wu, Carnegie Mellon University, Pittsburgh, United States. E-mail: albertwu87@gmail.com.

William Martin, Carnegie Mellon University, Pittsburgh, United States. E-mail: wmartin@cmu.edu.

Hartmut Geyer, Carnegie Mellon University, Pittsburgh, United States. E-mail: hgeyer@cs.cmu.edu.

Jonathan Hurst, Oregon State University, Corvallis, and Agility Robotics, Albany, Oregon, United States. E-mail: jonathan.hurst@oregonstate.edu.